Efficient Magnetic Field-Free Switching of a Symmetric Perpendicular Magnetic Free Layer for Advanced SOT-MRAM

Roberto L. de Orio[1], Alexander Makarov[2], Siegfried Selberherr[2], Wolfgang Goes[3], Johannes Ender[1], Simone Fiorentini[1], and Viktor Sverdlov[1]
[1]*Christian Doppler Laboratory for Nonvolatile Magnetoresistive Memory and Logic at the*
[2]*Institute for Microelectronics, TU Wien, Austria*
[3]*Silvaco Europe Ltd., Cambridge, United Kingdom*
{orio|sverdlov}@iue.tuwien.ac.at

***Abstract*—A long-standing problem of magnetic field-free switching of a symmetric perpendicular free layer by spin-orbit torque is resolved by employing two perpendicular consecutive current pulses. The optimal overlap of the second pulse line is found to be around 50%. The robustness of switching with respect to fluctuations of the second current pulse duration and of the overlap with the free layer is demonstrated.**

***Index Terms*—Spin-Orbit MRAM, perpendicular magnetization, magnetic field-free switching, two-pulse switching scheme**

I. Introduction

Spin-transfer torque magnetic RAM (STT-MRAM) is fast, possesses high endurance (10^{12}), and has a simple structure. It is compatible with CMOS technology and can be straightforwardly embedded in circuits [1]. It is particularly promising for use in IoT and automotive applications, as a replacement of conventional flash memory, as well as for embedded applications [2].

Although the use of STT-MRAM in last-level caches is possible [3], the switching current for operating at a speed faster than 10 ns is fairly high. The large current densities flowing through magnetic tunnel junctions lead to oxide reliability issues which in turn reduce the MRAM endurance. Thus, devices based on a new principle are required.

Spin-orbit torque (SOT) assisted switching of a free layer (FL) is promising, because it combines non-volatility, high-speed, and high-endurance [4]. In this memory cell the magnetic tunnel junction's (MTJ) free layer is grown on a material with a large spin Hall angle. The relatively large switching current is passing through a heavy normal metal (NM) wire on which the FL is grown [5]. The write current does not flow through the MTJ, while a much smaller read current is applied through the MTJ. This results in a three-terminal configuration where the read and write current paths are decoupled. Since the large write current does not flow through the oxide in the MTJ, this prevents the tunnel barrier from damage and improves device reliability. However, a static magnetic field is still required for deterministic switching [6] of the FL. Even though several paths to achieve a field-free switching were reported [7], [8], [9], these require a local intrusion into the cell fabrication, which makes large scale integration problematic.

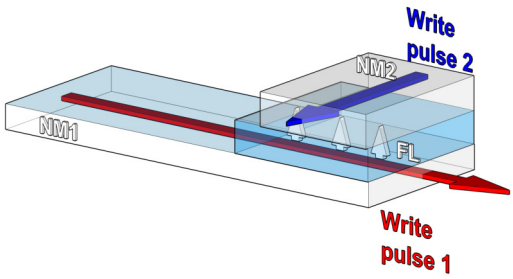

Fig. 1. Two-pulse switching scheme applied to the perpendicularly polarized square magnetic free layer (FL).

In this work we demonstrate that a magnetic field-free two-pulse switching scheme [10] previously proposed to switch a perpendicular FL of rectangular form is also suitable to switch a symmetric square FL. In contrast to the in-plane anisotropy field employed for deterministic switching of a rectangular FL, an in-plane stray magnetic field of a part of the square FL under the heavy normal metal NM2 wire (Fig. 1) acting on the rest of the FL is used to deterministically switch the symmetric FL. We also demonstrate that the switching scheme is robust with respect to the variations of the duration T_2 of the second pulse and fluctuations of the NM2 wire's partial overlap w_2 with the FL.

II. Two-Pulse Switching Scheme

The memory cell is shown in Fig. 1. The structure consists of a perpendicularly magnetized FL grown on top of a heavy metal wire (NM1) of $l = 3\,\text{nm}$ thickness. The FL fully overlaps with the NM1. Another heavy metal wire (NM2) also of $l = 3\,\text{nm}$ thickness lies on top of the FL. The parameters of the FL are listed in Table I. To guarantee a minimal thermal stability factor of 40, thus making the cell suitable for SRAM applications [11], we chose the FL dimensions $a \times a \times d = 25 \times 25 \times 2\,\text{nm}^3$, where a represents the width and length of the FL, and d its thickness. The NM1 has a width

TABLE I
PARAMETERS USED IN THE SIMULATIONS.

Saturation magnetization, M_S	4×10^5 A/m
Exchange constant, A	2×10^{-11} J/m
Perpendicular anisotropy, K	2×10^5 J/m^3
Gilbert damping, α	0.05
Spin Hall angle, θ_{SH}	0.3
Free layer dimensions	25×25×2 nm^3
NM1: $w_1 \times l$	25×3 nm^2
NM2: $w_2 \times l$	5 to 25×3 nm^2

$w_1 = a = 25$ nm, while NM2 wires of different widths, w_2, have been considered, so the NM2 can fully ($w_2 = a = 25$ nm) or partly overlap with the FL ($w_2 < a$).

The two-pulse switching scheme works as following: First, a pulse of a fixed duration $T_1 = 100$ ps and fixed current $I_1 = 200\,\mu$A, "Write pulse 1", is applied through the NM1. This results in a current density of 2.7×10^{12} A/m^2. Then, a second consecutive perpendicular pulse is applied through the NM2. This pulse, "Write pulse 2", has a current of $I_2 = (w_2/a)200\,\mu$A, which yields the same current density (2.7×10^{12} A/m^2) as "Write pulse 1". However, the "Write pulse 2" has a variable duration T_2, so the effect of different pulse configurations on the switching dynamics of the device is investigated.

III. Modeling

The magnetization dynamics of the magnetic system is described by the Landau-Lifshitz-Gilbert equation [12].

$$\frac{\partial \mathbf{m}}{\partial t} = -\gamma \mathbf{m} \times \mathbf{H_{eff}} + \alpha \mathbf{m} \times \frac{\partial \mathbf{m}}{\partial t} + \frac{1}{M_S}\mathbf{T_S} \qquad (1)$$

$\mathbf{m}$ is the position-dependent magnetization $\mathbf{M}$ normalized by the saturation magnetization M_S, γ is the gyromagnetic ratio, α is the Gilbert damping, and $\mathbf{H_{eff}}$ is an effective magnetic field. $\mathbf{T_S}$ is the spin torque caused by the current pulses and is given by

$$\mathbf{T_S} = +\gamma \frac{\hbar}{2e}\frac{\theta_{SH} I_1}{dw_1 l}\left[\mathbf{m} \times (\mathbf{m} \times \mathbf{y})\right]\Theta(t)\Theta(T_1 - t) \qquad (2)$$
$$-\gamma \frac{\hbar}{2e}\frac{\theta_{SH} I_2}{dw_2 l}\left[\mathbf{m} \times (\mathbf{m} \times \mathbf{x})\right]\Theta(t - T_1)\Theta(T_2 + T_1 - t),$$

where e is the elementary charge, $\hbar$ is the Plank constant, and θ_{SH} is an effective Hall angle. The effective field $\mathbf{H_{eff}}$ includes the exchange, uniaxial perpendicular anisotropy, demagnetization, and random thermal field at 300 K. To describe the magnetization dynamics, we employ our in-house open-source tool [13], [14] based on the finite difference discretization method. The values of the parameters used in the simulations are given in Table I.

IV. Results

In the case of full overlap of the NM2 with the FL, i. e. $w_2 = 25$ nm, no "Write pulse 2" parameters were detected which would support deterministic switching of the FL. Fig. 2 shows the magnetization components of some sample realizations out of 20 runs of such a case. Initially, the "Write pulse 1" puts the magnetization in the plane of the FL ($m_z = 0$). Then, the "Write pulse 2" puts the magnetization of the whole FL along the the $-x$ direction ($m_x = -1$). However, after the pulse is removed, the magnetization returns to the initial $+z$ direction, as shown by the realizations of m_z.

This is in contrast to the SOT-MRAM cell with a rectangular

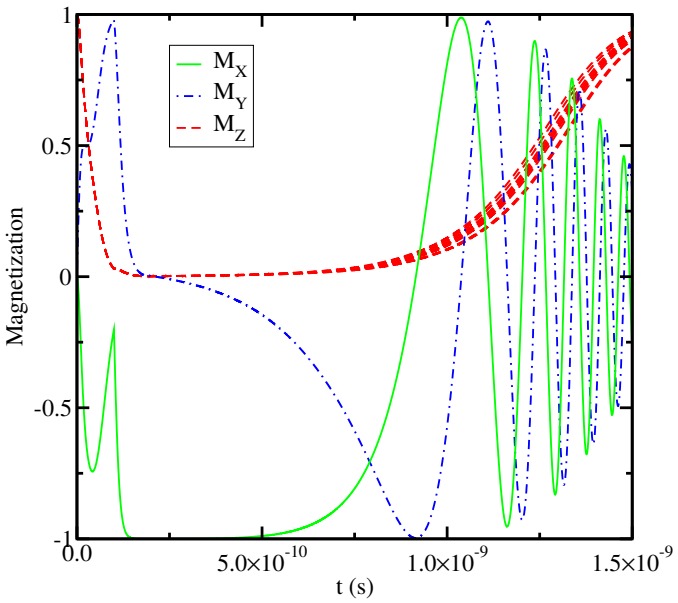

Fig. 2. Magnetization components for several realizations for structures with $w_2 = 25$ nm and $T_2 = 80$ ps. No "Write pulse 2" parameters were detected which support deterministic switching of the FL.

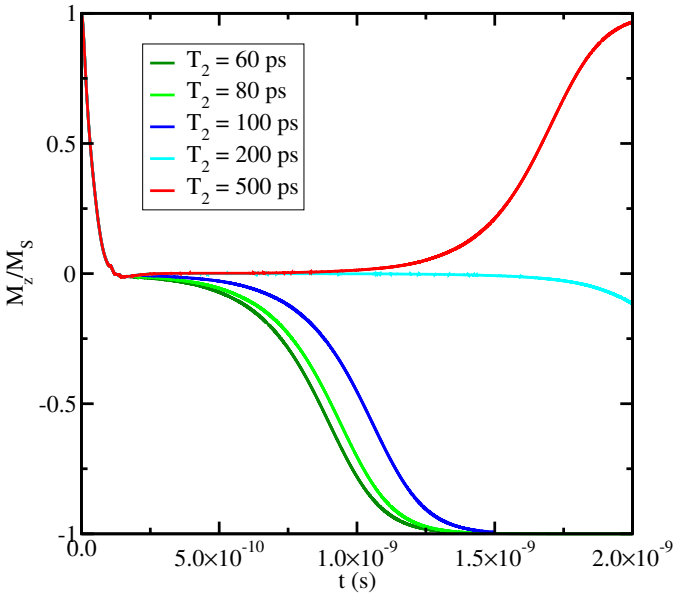

Fig. 3. Average of 20 switching realizations. For partial overlap $w_2 = 17.5$ nm, reliable switching for square FL at short "Write current 2" pulses duration (T_2) appears.

layer, where the shape anisotropy played the role of the external magnetic field, while the switching direction was determined by the polarity of the "Write pulse 2" which pushes the magnetization to one or another side from the in-plane direction along the short side of the rectangle [10]. As there is no uniaxial shape anisotropy for a square FL, the switching is unreliable for the full overlap, as shown in Fig. 2.

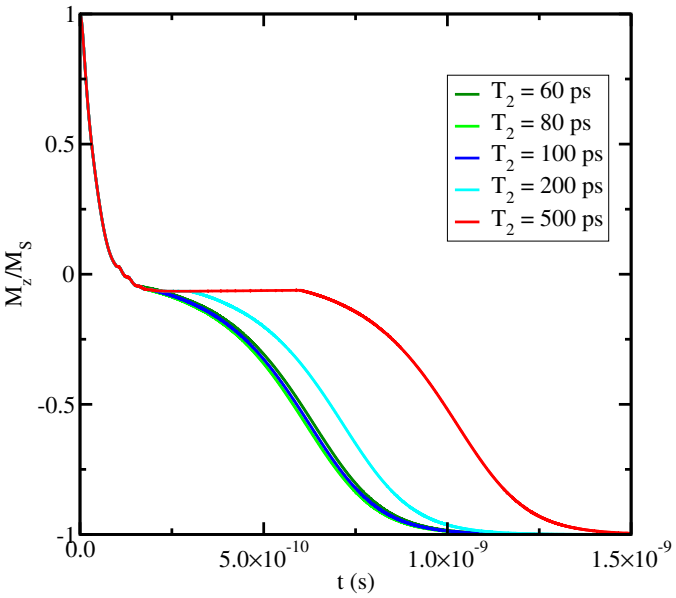

Fig. 4. Average of 20 switching realizations for $w_2 = 10\,\text{nm}$. Reliable switching is observed for all T_2.

Surprisingly, when the NM2 overlap with the FL is reduced to $w_2 = 17.5\,\text{nm}$, deterministic switching is observed for all 20 realizations, if the duration of "Write pulse 2" becomes shorter than 200 ps, as shown in Fig. 3. If now the overlap w_2 is further reduced below 15 nm, the switching becomes deterministic for all pulse durations T_2 considered. Fig. 4 shows the average over 20 realizations for time dependencies of magnetization switching, for $w_2 = 10\,\text{nm}$ and several T_2. One can see that for a "Write pulse 2" with duration in the range $60\,\text{ps} \leq T_2 \leq 100\,\text{ps}$ the curves nearly coincide.

Fig. 5 demonstrates the typical position dependent magnetization just after the write pulses are applied. After the "Write pulse 1" is turned on, the magnetization is placed in the plane of the FL along the y direction, as suggested by the first torque term in (2). Then, the magnetization under the NM2 gets rotated due to the SOT of the second pulse (second torque term in (2)), which is shown in Fig. 5 for an NM2 of $w_2 = 10\,\text{nm}$, thus partially overlapping with the FL. This creates a stray field of the magnetization under the NM2, which acts as an effective in-plane magnetic field for the rest of the FL. As a consequence, the field causes the magnetization to precess away from its in-plane orientation, as shown in Fig. 6. The whole magnetization of the FL precesses in the same sense, if the "Write pulse 2" is short, which is the reason of the switching scheme's robustness with respect to T_2 fluctuations around $T_2 = 80\,\text{ps}$.

Fig. 7 shows a comparison between the magnetization dynamics for structures with different overlaps between the NM2 and the FL for a "Write pulse 2" of $T_2 = 80\,\text{ps}$. The shortest switching time (taken at the time when $M_Z/M_S = -0.5$) of

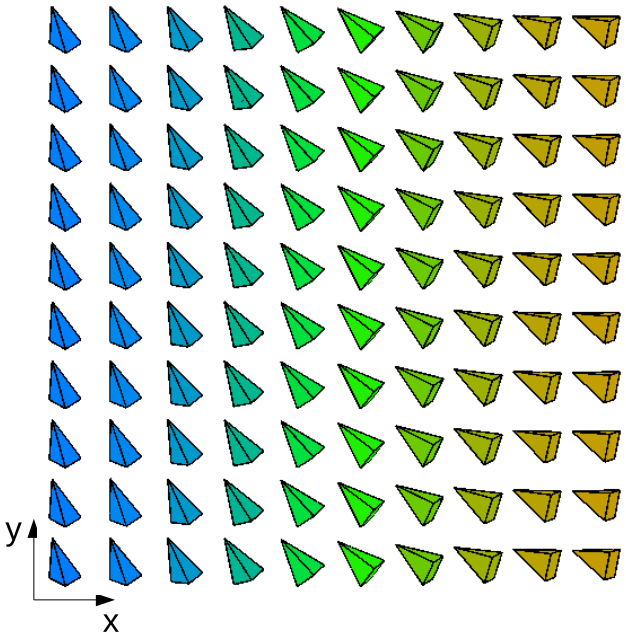

Fig. 5. Snapshot of magnetization for $w_2 = 10\,\text{nm}$ just after "Write pulse 2" is on.

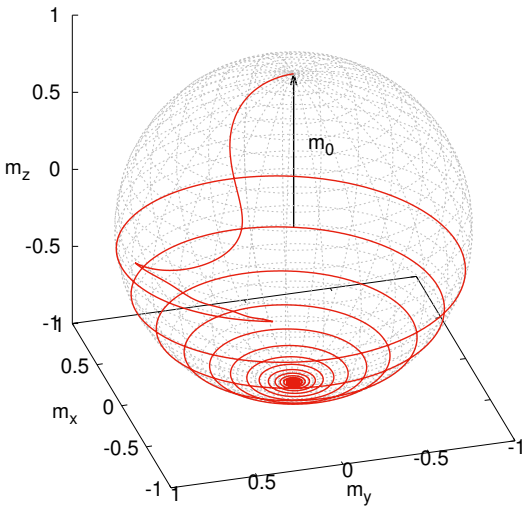

Fig. 6. Magnetization switching path for the structure with $w_2 = 10\,\text{nm}$ and "Write pulse 2" with $T_2 = 80\,\text{ps}$. $\mathbf{m_0}$ represents the initial magnetization.

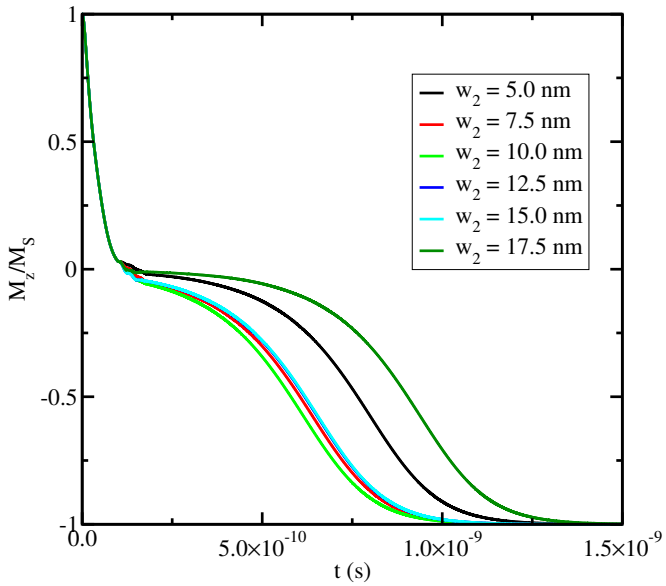

Fig. 7. Comparison of the magnetization switching for different overlaps between the NM2 and the FL for a "Write pulse 2" of $T_2 = 80\,\text{ps}$.

about 0.6 ns is observed for $w_2 = 10\,\text{nm}$, while the largest switching time, 0.9 ns, is measured for $w_2 = 17.5\,\text{nm}$, the structure with the biggest overlap between the NM2 and the FL (for which deterministic switching happens). It is interesting to note that the switching times are very close to the minimum value of 0.6 ns for NM2 widths in the range $7.5\,\text{nm} \leq w_2 \leq 15\,\text{nm}$.

Fig. 8 summarizes the switching times as a function of the NM2 width and pulse duration. It clearly shows that for $T_2 \leq 100\,\text{ps}$ and for $7.5\,\text{nm} \leq w_2 \leq 15\,\text{nm}$ the switching time is minimum and almost the same, thus indicating the robustness of the two-pulse approach.

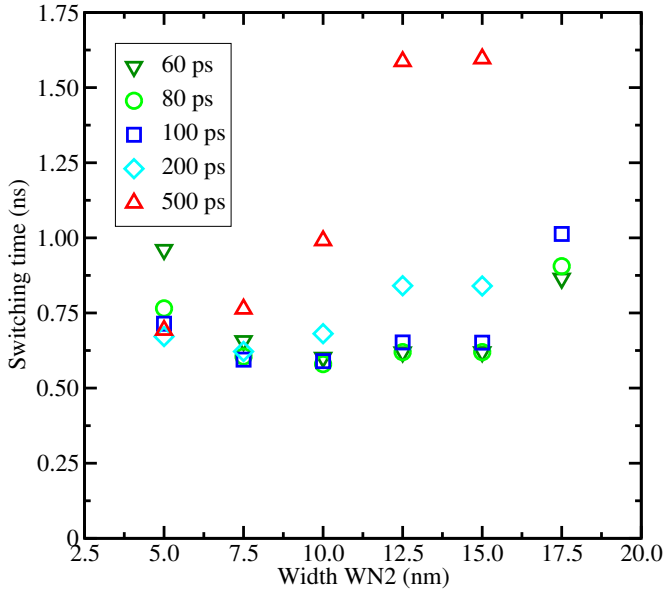

Fig. 8. Switching time as function of w_2 for several T_2.

V. Conclusion

Magnetic field-free switching of a symmetric perpendicular free layer by spin-orbit torque is resolved by employing two perpendicular consecutive current pulses. The structure has a second pulse line which partially overlaps with the free layer. The optimal overlap is found to be around 50%. A short switching time of 0.6 ns has been obtained. The switching remains practically the same for devices with dimensions $w_2 = 11 \pm 4\,\text{nm}$ and for a duration of the second pulse in the range $T_2 = 80 \pm 20\,\text{ps}$. This proves that the two-pulse switching scheme is very robust to fluctuations of both, the second pulse duration and the overlap with the free layer.

Acknowledgment

The financial support by the Austrian Federal Ministry for Digital and Economic Affairs and the National Foundation for Research, Technology and Development is gratefully acknowledged.

References

[1] D. Apalkov, B. Dieny, and J. Slaughter, "Magnetoresistive Random Access Memory," *Proc. of the IEEE*, vol. 104, pp. 1796–1830, 2016.

[2] O. Golonzka, J.-G. Alzate, U. Arslan, M. Bohr, P. Bai, J. Brockman *et al.*, "MRAM as Embedded Non-Volatile Memory Solution for 22FFL FinFET Technology," in *Proc. of the 2018 IEDM*, 2018, pp. 18.1.1–18.1.4.

[3] G. Jan, L. Thomas, and S. Le, "Achieving Sub-ns Switching of STT-MRAM for Future Embedded LLC Applications through Improvement of Nucleation and Propagation Switching Mechanisms," in *Proc. of the 2016 Symp. VLSI Technology and Circuits*, 2016, pp. 1–2.

[4] S.-W. Lee and K.-J. Lee, "Emerging Three-Terminal Magnetic Memory Devices," *Proc. of the IEEE*, vol. 104, pp. 1831–1843, 2016.

[5] I. M. Miron, K. Garello, G. Gaudin, P.-J. Zermatten, M. V. Costache, S. Auffret *et al.*, "Perpendicular Switching of a Single Ferromagnetic Layer Induced by In-plane Current Injection," *Nature*, vol. 476, pp. 189–193, 2011.

[6] S.-H. C. Baek, V. P. Amin, Y.-W. Oh, G. Go, S.-J. Lee, G.-H. Lee *et al.*, "Spin Currents and Spin-Orbit Torques in Ferromagnetic Trilayers," *Nature Materials*, vol. 17, pp. 509–513, 2018.

[7] G. Yu, P. Upadhyaya, Y. Fan, J. G. Alzate, W. Jiang, K. L. Wong *et al.*, "Switching of Perpendicular Magnetization by Spin-Orbit Torques in the Absence of External Magnetic Fields," *Nature Nanotechnology*, vol. 9, pp. 548–554, 2014.

[8] A. van den Brink, G. Vermijs, A. Solignac, J. Koo, J. T. Kohlhepp, H. J. M. Swagten *et al.*, "Field-Free Magnetization Reversal by Spin-Hall Effect and Exchange Bias," *Nature Communications*, vol. 7, p. 10854, 2016.

[9] Y.-C. Lau, D. Betto, K. Rode, J. M. D. Coey, and P. Stamenov, "Spin-Orbit Torque Switching without an External Field using Interlayer Exchange Coupling," *Nature Nanotechnology*, vol. 11, pp. 758–762, 2016.

[10] V. Sverdlov, A. Makarov, and S. Selberherr, "Reliable Sub-Nanosecond Switching of a Perpendicular SOT-MRAM Cell without External Magnetic Field," *Journal on Systemics, Cybernetics and Informatics*, vol. 16, pp. 55–59, 2018.

[11] K. Ikegami, H. Noguchi, S. Takaya, C. Kamata, M. Amano, K. Abe *et al.*, "MTJ-Based Normally-Off Processors with Thermal Stability Factor Engineered Perpendicular MTJ, L2 Cache Based on 2T-2MTJ Cell, L3 and Last Level Cache Based on 1T-1MTJ Cell and Novel Error Handling Scheme," in *Proc. of the 2015 IEDM*, 2015, pp. 25.1.1–25.1.4.

[12] S. Lepadatu, "Unified Treatment of Spin Torques using a Coupled Magnetisation Dynamics and Three-Dimensional Spin Current Solver," *Sci. Rep.*, vol. 7, p. 12937, 2017.

[13] A. Makarov, "Modeling of Emerging Resistive Switching Based Memory Cells," Ph.D. Dissertation, Institute for Microelectronics, TU Wien, Vienna, 2014.

[14] (2016) ViennaMag. www.iue.tuwien.ac.at/index.php?id=24.